Advanced Course and Workshop on Blood Flow
BF 2005 – (pp.135–162) – Warsaw, 2005.

Flow in Artificial Valves and Blood Pumps

Klaus Affeld, Deibris Aguilera, Perrine Debaene, Leonid Goubergrits, Ulrich Kertzscher, and Tobias Timmel

Biofluidmechanics Laboratory
Charitè, Universitätsmedizin Berlin,
Spandauer Damm 130,
14050 Berlin, Germany
klaus.affeld@charite.de

A variety of impairments and diseases require the implantation of mechanical elements in the circulatory system. The ones most difficult to design are artificial valves and artificial blood-pumps. Blood can be considered as a Newtonian fluid under certain conditions. The greatest problem is caused by the tendency of the blood to form solid particles, called clots. Such clots are generated through the interaction of three qualities: of blood, of the wall, and finally of the flow. The latter is the one the fluiddynamicist can actively influence by avoiding flow separations. These are experimentally and numerically investigated and examples for unfavourable and for favourable designs are given.

Key words: *Blood flow, flow separation, artificial valves, thrombus generation*

1. Introduction

A variety of impairments and diseases require the implantation of mechanical elements in the circulatory system. The ones most difficult to design are artificial valves and artificial blood-pumps. The greatest difficulty arises, in that there is no material which can truly mimic the inner wall of the circulatory system. This wall is covered with specialized cells—the endothelium. Unimaginable for the engineer, each of the cells contains a flow sensor, which senses the shear stress of the flow. The cell orients itself to the flow, it gives a signal—nitric oxide—to the platelets to calm down and not to adhere [1]. This wonderful mechanism is absent when artificial materials are used, such as metals, polymers, ceramics, pyrolitic carbon or others. The engineer has

to try to create a good design which avoids just this stall and lowers shear stress. He will not come up with a valve that is as good as a healthy one, but one which is better than the diseased valve. The same is true, however to a much lesser degree, for the artificial blood pumps which have the objective to assist or even to replace the natural heart.

2. Blood as a Newtonian Fluid

Newton's famous formula (Fig. 1) combines the shear-stress of a fluid with the shear rate. Consequently, all fluids behaving according to this formula are called Newtonian fluids. But is blood such a fluid? More than 40 % of it consists of cells, which at times accumulate to form "rouleaux" (Fig. 2). These rolls cling together and at low shear rates the blood even resembles a solid. When sheared, blood becomes less viscous, and at high shear rates it behaves as a Newtonian fluid.

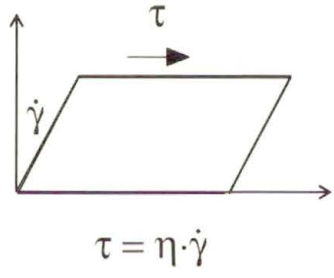

FIGURE 1. Newton's insight—his ingeniously simple formula enables us to compute most technical flows. Is it applicable to the special fluid, blood?

In the body, the blood is subjected to quite high shear-stress (Fig. 3). In the capillaries of various species, including humans, we encounter wall shear rates of up to ten thousand 1/s. In the vena cava, which is the central vessel with the slowest blood flow, we still encounter a wall shear rate of about 50 1/s. Above the point where this wall shear rate is reached, blood behaves as a Newtonian fluid [2]. At lower shear rates rouleaux formation can be observed. Typically, they take between ten to sixty seconds to form. From this follows that Newton's formula can be applied to all practical computations.

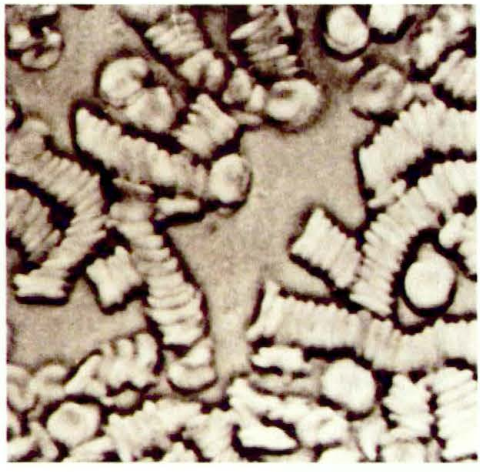

FIGURE 2. When not in motion, red blood cells attach to each other and form rouleaux. Blood becomes more viscous; almost a fragile solid.

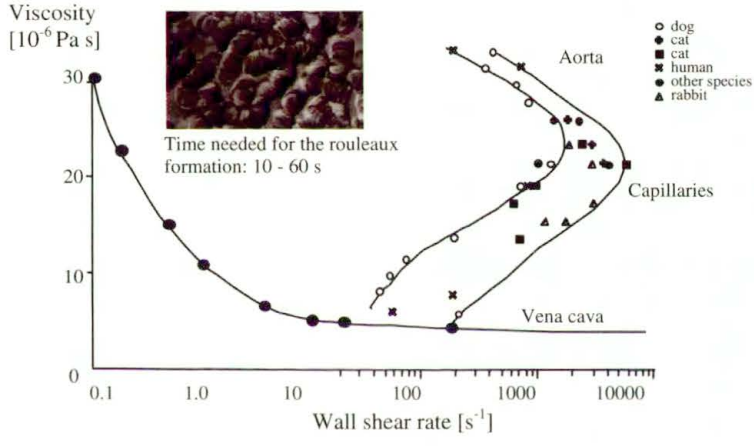

FIGURE 3. Blood becomes a non Newtonian fluid if it has 10 to 60 seconds to rest in a low shear rate zone. However, within the healthy body no such zone exists, as shown in the graph on the right side. The ordinate here denotes the position of the vessel in the body, [15].

3. The Role of Flow Separations

Only under pathological flow conditions is the time necessary for rouleaux formation given. An example of such flow conditions are flow separations. For instance, the flow over an air foil (Fig. 4) separates, as shown by Prandtl in his flow visualization experiments. In the case of an air foil, the flow separation

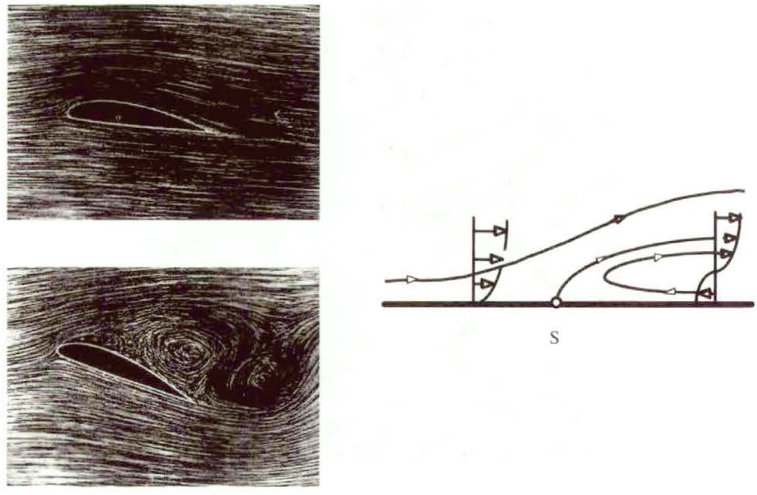

FIGURE 4. Attached flow around an air foil and flow separation at a higher angle of attack, as shown in Prandtl's famous flow visualization experiments. The right side shows a diagrammatic cross section through a flow separation.

results in the loss of lift and may induce the airplane to crash, causing many fatalities.

In the blood stream, flow separations also occur. They are not necessarily fatal, but if they endure, are dangerous to the patient. A schematic diagram of a flow separation can be seen in Fig. 4 (right side). At the stagnation point the flow detaches and a separation bubble may form. Within the separation bubble the blood circulates slowly, rouleaux formation may take place, and in addition, platelets are able to aggregate in the vicinity of the stagnation point. These adhered platelets emit thromboactive substances, which cause more platelets to be attracted until a thrombus is finally formed.

In this way, a connection between the flow of blood and thrombus generation may be observed. This was first observed by the eminent pathologist Rudolf Virchow, who published his findings as early as 1856 [3], see Fig. 5. During his many post-mortems, he observed thrombi and atherosclerotic alterations of the vessel wall at specific locations, especially at bifurcations. When a blood vessel bifurcates the blood velocity is decreased and in many cases flow separation occurs naturally. As new studies have shown, persistent low shear stress at the vessel wall modifies the endothelial cell layer, which transforms into smooth muscle cells and lipids [4]. In this way, fatty streaks develop which are the precursor of the atherosclerotic plugs which

FIGURE 5. Virchow's triad shows a functional connection between the qualities of the blood, the vessel wall and the flow.

were observed by Virchow. Intuitively, he then formulated a triad of three entities:

- quality of the blood (activated platelets, lipids)
- quality of the flow (smooth flow along the wall, detached flow)
- quality of the wall (healthy endothelial cells, atherosclerotic plugs, artificial material)

Figure 6 shows some examples: atherosclerotic lesions on the inner side of the aorta and a thrombus at the metal ring of an artificial cardiac valve.

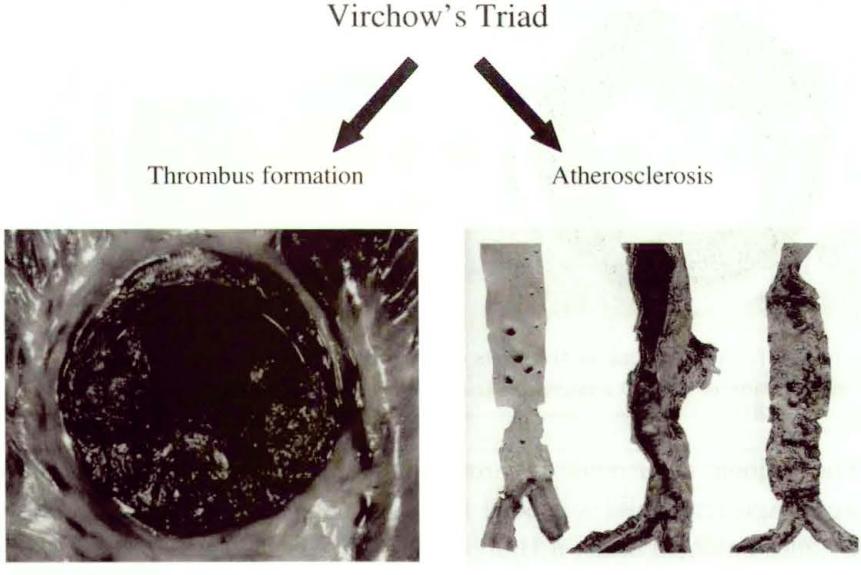

FIGURE 6. The result of a mismatch of blood, wall and flow: a thrombus at an artificial valve and a degeneration of the natural aortic wall.

The artificial materials which are at our disposal are all far inferior compared to the endothelial cells. All artificial materials may be considered thrombogenic. However there are materials which are a compromise between an artificial and the natural vessel wall. These materials are bioprosthetic materials, of which one example is the pericardium. This material is slightly cross-linked. It loses its immunological properties, but retains many mechanical properties. In that way, the tissue from a different species, for example the cow, may be harvested and sutured into a cardiac valve for a human. These valves do not require anticoagulants, and are therefore implanted in high numbers [5].

4. Flow Through Valves

Virchow's analysis indicates that there must be a delicate balance of the three above mentioned qualities. A thrombus can form if the quality of the flow is disturbed, as shown in Fig. 7. It shows a large thrombus at the edge of a bioprosthetic valve that had been used in a ventricular assist device [6]. A cross-section of a CFD (computational fluid dynamics) simulation shows an area of very slow blood flow in the sinuses of the valve duct.

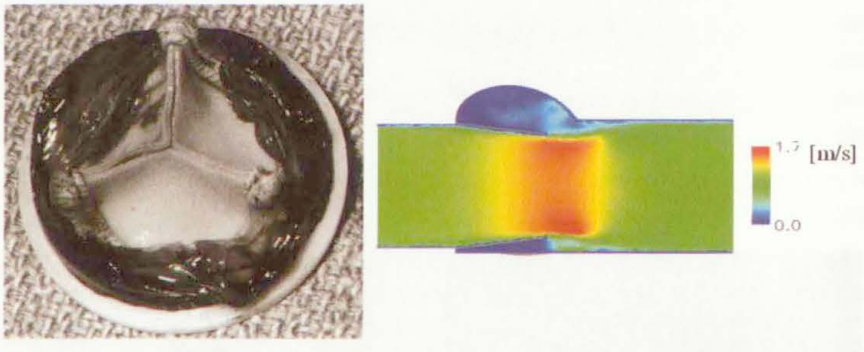

FIGURE 7. A thrombus at the sinus of a pericardial valve for a VAD (left). The cross-section of a CFD simulation (right) shows a low velocity in the sinus.

The frequent occurrence of thrombi in artificial heart valves was the reason to design and build a special flow channel. This flow channel uses, at a ten times enlarged scale, a Björk-Shiley valve, which had previously been transformed into a model with a 200 mm diameter, see Fig. 8. The advantage of this up scaling—keeping the Reynolds number similarity—is that the velocities are greatly reduced and the flow field is larger. Fine details of the

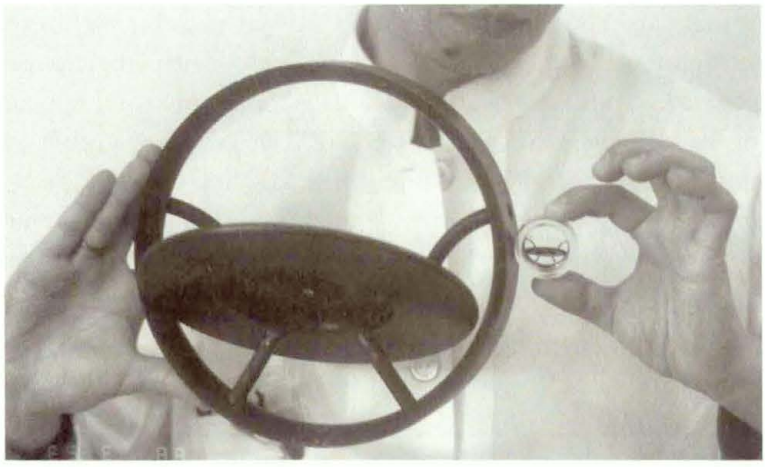

FIGURE 8. An enlarged model of the Björk-Shiley valve is shown and compared to the original.

flow are revealed. A schematic diagram is shown in Fig. 9. The fluid, water, is driven by a computer controlled axial flow pump which simulates the physiological aortic flow curve. The total volume is 600 liters. A whole cardiac cycle lasts several minutes and the fluid velocities are below ten centimeters per second, which is a precondition for effective flow visualization [7, 8].

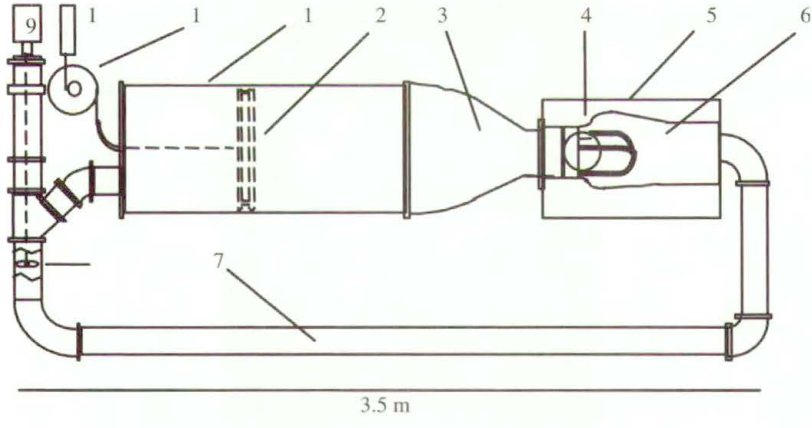

FIGURE 9. Water tunnel for 10:1 scaled up valve models. The flow is non-stationary, keeps the Reynolds-number similarity and as a result is very slow. The time expansion is about 200 fold. 1. tank, 2. piston, 3. contraction, 4. test valve, 5. observation tank, 6. aortic root, 7. return duct, 8. axial flow pump, 9. motor, 10. displacement transducer, 11. gear.

To visualize the flow through the heart valve, the water within the model of the aortic root is mixed with dye and illuminated with a light sheet. When the systolic flow is initiated, water enters the aortic valve and appears black. It more or less displaces the dyed water and makes the flow visible. Figure 10 shows a model of a tri-leaflet valve and Fig. 11—flow through such a valve. The entering flow forms a central jet, which barely mixes with the fluid in the aortic root. The fluid in the vicinity of the valve ring is not mixed at all. The flow simulates the blood flow through the valve shown in Fig. 7, and thus gives an explanation for the large thrombus. Figure 12 shows the flow through a Björk-Shiley valve. After opening, a flow separation is formed at the trailing edge of the occluder. One side of the valve ring is well rinsed—it appears completely black—while the flow is stagnant on the upper side. As a result a thrombus generation is likely at this site, and in fact the thrombus in Fig. 6 is exactly in this region. Figure 13 shows yet another valve—the St. Jude valve. It is a bi-leaflet valve with two occluders, which open like double-doors. The light sheet is parallel to the door axis and cuts through the middle of the flow channel. A turbulent jet is formed. However, a slow rinsing of the valve ring is also observed here.

FIGURE 10. 10:1 model of a polyurethane tri-leaflet valve

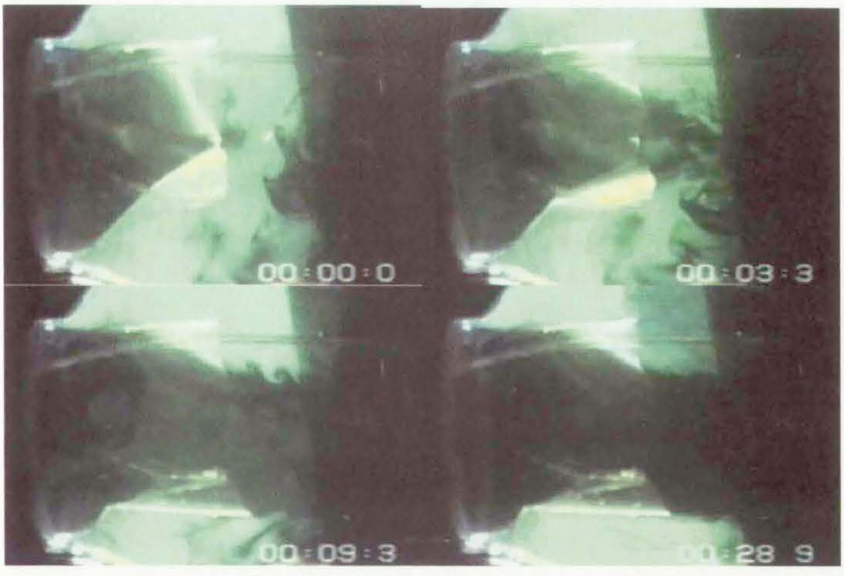

FIGURE 11. 10:1 model of a tri-leaflet valve during various phases of the systolic flow. The water in the aortic root is dyed and appears green. The water from the new systole is not dyed and appears black. This makes the washout visible.

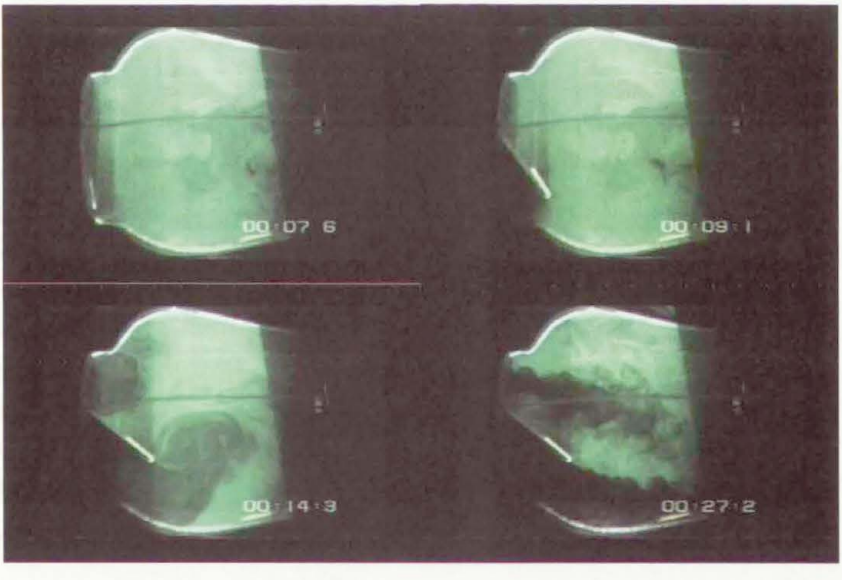

FIGURE 12. 10:1 model of the Björk-Shiley valve. A large flow separation appears at the trailing edge of the occluder. The fluid at the ring remains stationary.

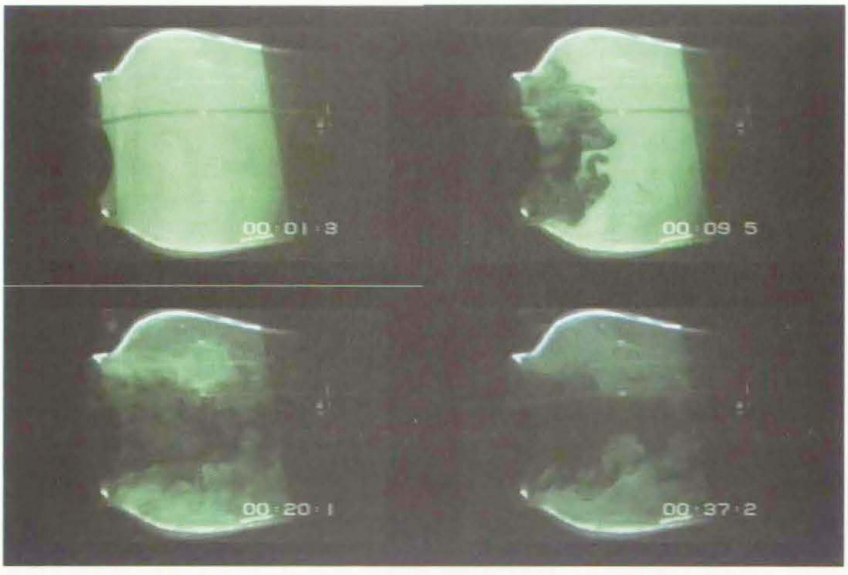

FIGURE 13. 10:1 model of the St. Jude valve. A turbulent jet forms in the middle. The fluid at the ring remains stationary.

5. New Valve Design

All of these experiments show that, in these models of artificial heart valves, flow separations are always present. Is it possible to design a valve without flow separations? The answer is probably not; at least it hasn't been achieved yet. The reason for this is that the aortic root is a vessel which acts as a diffuser. In other words, a jet enters a diverging vessel. This means that the flow is decelerated, and the pressure upstream is higher than the pressure downstream. In the boundary layer this has the effect that the flow is easily reversed and a flow separation takes place, as shown in Fig. 4.

The situation with the diverging channel, however, is not valid for an artificial valve in a ventricular assist device (VAD). In this case the engineer has full control over the design of the channel.

5.1. S-Valve

An example of a possible design, here a duct with an s-shaped center line, is shown in Fig. 14. The objective of this design is to avoid a flow separation, which may be seen in Fig. 12. The occluder (9) has a minimal angle of attack

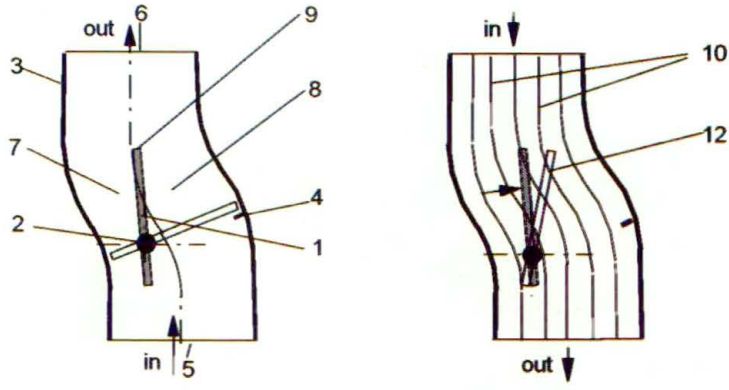

FIGURE 14. A schematic diagram of the S-Valve. Objective of this design is to avoid flow separation at the occluder.

to the incoming flow, which is labeled with the arrow (5) in the diagram. This is also true for the flow at the trailing edge. For the flow, this connotes an acceleration in area (8), and a deceleration in area (7). When the flow reverses (Fig. 14, right) in the first instance, friction does not play a role. The stream lines resemble that of a potential flow. In this way, they attack the occluder at an angle and also initiate the rotation around the axis. As a result, it moves from position (12) to full closure at (4). Had one placed the occluder in a straight duct, the stream lines at the initiation of the closure would be parallel to the occluder in the open position, and the valve would not close. With the s-shaped duct however, flow separation can be avoided, and closure times comparable to the normal Björk-Shiley valve can be achieved [9, 10].

The design of the duct with an otherwise unchanged Björk-Shiley valve is shown in Fig. 15. The CFD computation of the flow in an S-Valve, in comparison to the Björk-Shiley valve in a straight cylindrical duct, is depicted in Fig. 16.

Figure 17 shows a view of the wall shear stress of the same flow. The wall shear stress has very low values near the ring in the cylindrical duct, as well as in a large area downstream near the lower wall. In the S-Valve near the ring, the wall shear stress is much higher because the ring is integrated into the wall. Also, the area of wall shear stress is reduced downstream from the occluder. Figure 18 shows the washout process of the S-Valve in the large water channel. In accordance to the CFD studies only small flow separations appear.

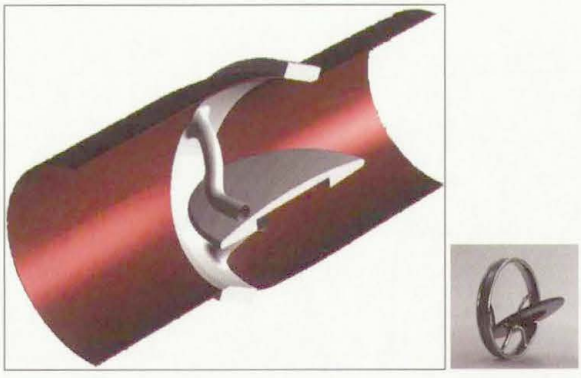

FIGURE 15. A view of a CAD model of an S-Valve. For practical purposes, it is a Björk-Shiley valve in a special duct.

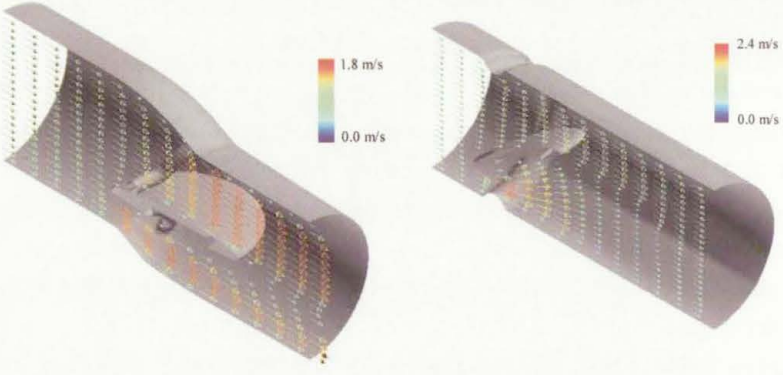

FIGURE 16. Comparison between the CFD flow field around an occluder in an S-shaped duct and in a straight duct.

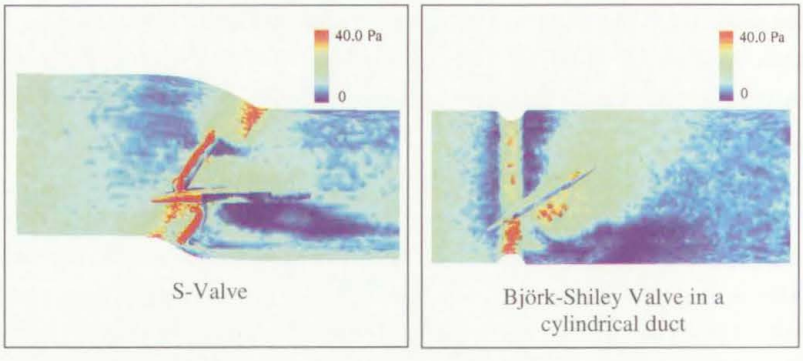

FIGURE 17. A comparison between the Wall shear stress of the two different arrangements.

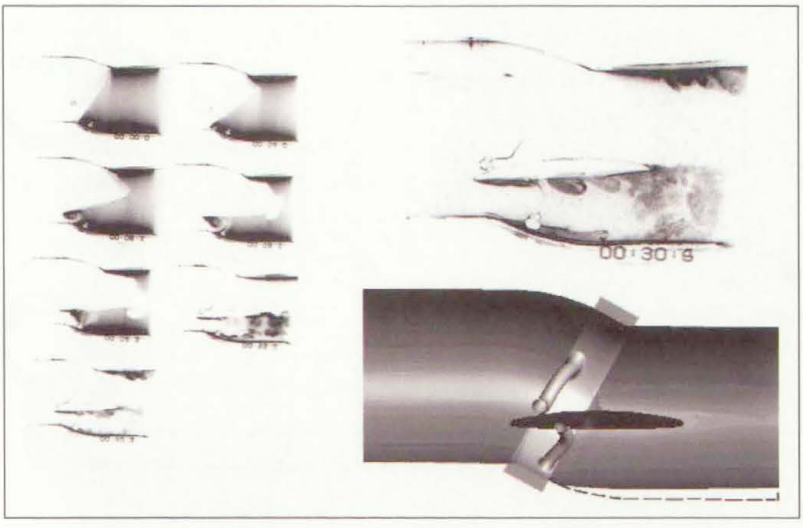

FIGURE 18. A washout experiment of the S-Valve in the large water tunnel.

These computations were tested in the above mentioned water channel in an enlarged 10:1 scale model. Large flow separations are absent; however, small areas of flow separation appear at the upper and lower walls of the duct and on the lower side of the occluder. This occurs during a time span of 30 seconds (enlarged model), which corresponds to a real-time of 6 milliseconds in the real model. Since 6 milliseconds comprises of only a small section of the systolic time of 300 milliseconds, a complete washout during this time span is achieved.

5.2. Purge Flow Valve

Yet another idea to increase the washout is pursued using the valve shown in Fig. 19. It is a mono-leaflet valve with a sinus [11]. When the valve opens, a part of the main flow impinges on a flow divider, which directs a part of the main flow into the sinus. In this way a purge flow is generated which greatly reduces the washout time. In a CFD study, shown in Fig. 20, a systematic variation of geometric parameters was performed. From 188 possible parametric combinations, 34 were selected and studied with the help of CFD [12]. The objective was to minimize the area of low wall shear stress. Figure 21 shows an example of the wall shear stress inside the sinus. From these results, 4 valves were selected, fabricated, and tested in a dye washout experiment.

IDEA:

Accept flow recirculation, but wash out critical regions periodically.

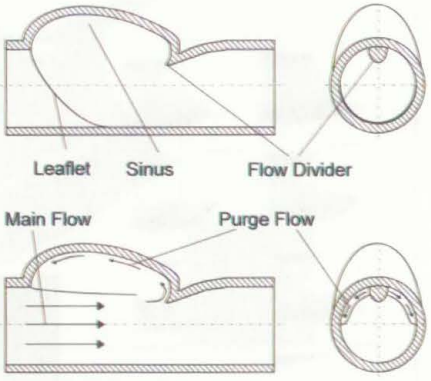

FIGURE 19. A schematic cross section of the purge flow valve.

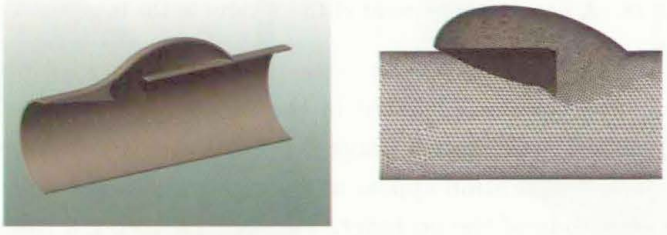

FIGURE 20. Variation of parameters which define a mono-leaflet purge flow valve.

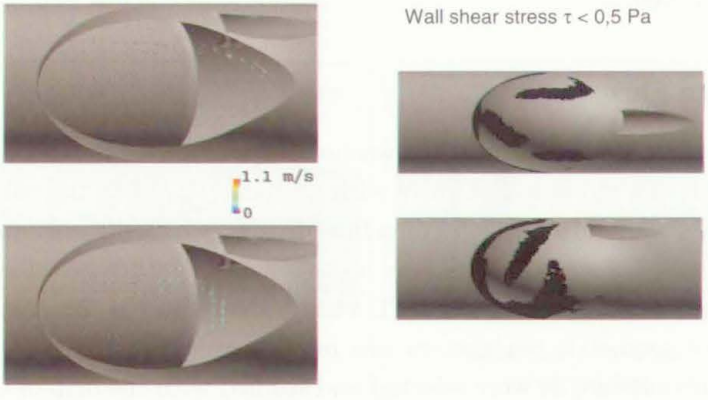

FIGURE 21. Wall shear stress as a function of different parameters.

The diagram (Fig. 22) shows that one valve has a faster washout and thus has superior qualities in comparison to the others. This technology can also be applied to a tri-leaflet valve, as is shown in Fig. 23.

Systematic variation of geometric parameters

- 188 possible parametric combinations
- Design of only 34 models (Taguchi method—Quality Management)

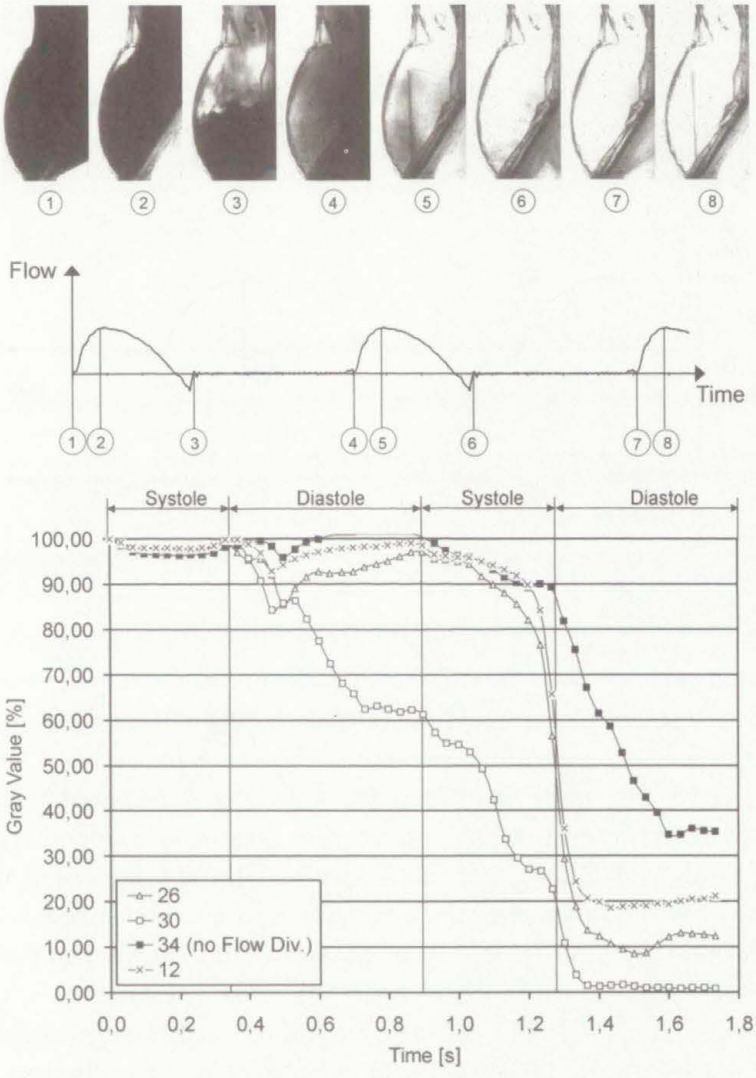

FIGURE 22. Results of wash out experiments of 4 different valves.

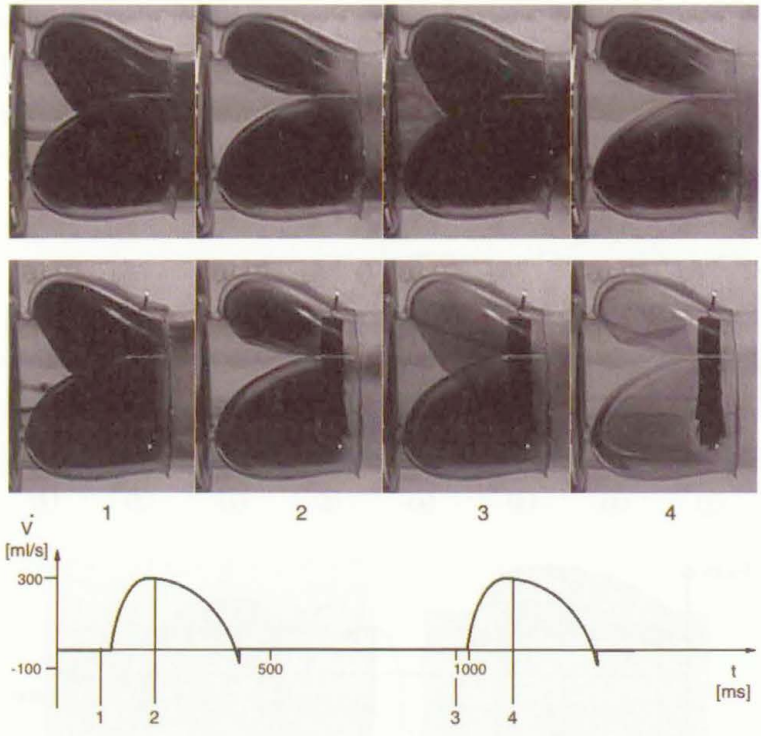

FIGURE 23. Washout experiment in a tri-leaflet valve without (above) and with purge flow (below).

5.3. Ball Valve

Another valve was also investigated, which applies a sphere as an occluder. Such valves were developed and implanted in great numbers during the early days of artificial heart valve implantations. Some, as for instance the Starr-Edwards valve, were quite successful, and worked in some patients for longer than 25 years. However, in many patients it did create a considerable pressure drop if the individual anatomy of this patient did not work well with the ball, which in the open position protrudes into the aortic root. Thus an individual match of the geometry of the valve and the patient's anatomy was a precondition for the success of the valve. As a result of this, different valve designs comprising of a flat disc instead of a ball were introduced. An example of such a valve is the Björk-Shiley valve, which was discussed above. The ball as a blunt body causes quite a resistance and large flow separations in its wake. This is true for a ball in an open space and also in a duct with

a geometry which is not matched to the ball, as was the case in most of the patients receiving Starr-Edwards valve.

6. Flow Through a Ventricular Assist Device (VAD)

However, this situation changes completely if one designs a ball valve for a VAD. Instead of the human anatomy, one has full control over the geometry of the duct. A ball moving through open space experiences large flow separations on the trailing side, because the fluid cannot follow the curvature of the ball. The flow beyond the greatest diameter is decelerated, thus creating the conditions for the flow separation. However, if a duct can be applied, its geometry can be designed so that the flow behind the largest diameter is accelerated. The outflow area of the duct is thus larger than the inflow area and the acceleration of the fluid leads to a pressure drop. This is the price which has to be paid for the absence of flow separation at the duct wall. However there remains one stagnation point downstream of the ball and this area creates a flow separation. Since the ball can move freely, it rotates a little bit with every pulse. As a result, the flow separation is always at a different location of the ball surface. This was investigated in a CFD model (Fig. 24) and by a variation of geometric parameters we managed to minimize areas of low shear stress.

In Fig. 25, the engineering solution of this valve, the guidance of the ball and the systolic stop are integrated into the housing, and a smooth inner surface without steps could be created. Figure 26 shows a sequence of a dye washout experiment in a large water channel. After a few milliseconds, a complete washout of the wall region has been attained.

Figure 27 shows yet another experiment: the flow inside a real-sized valve was assessed with Particle Image Velocimetry (PIV). The flow field agrees well with the other experimental methods. Also, Fig. 28 shows how such ball valves are integrated into a VAD, which in this case is a pneumatically driven blood pump. The inner surface is fabricated in halves including the valves and the flexible diaphragm.

Later, the balls are inserted and the two halves are joined to form one blood pump, which is shown in Fig. 29. The flow inside such a blood pump, which was assessed with PIV, is shown in Fig. 30. Shown is a circular flow with a jet from the inflow valve. The outflow takes place without flow separation. A more complicated flow is shown in Fig. 31. In this case the inflow

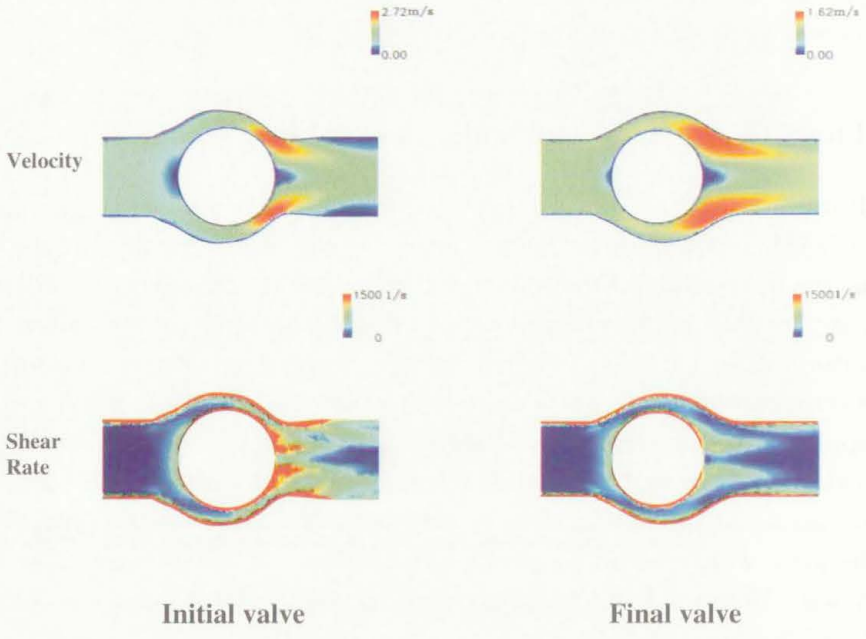

FIGURE 24. CFD results of flow through ball valves with different geometries.

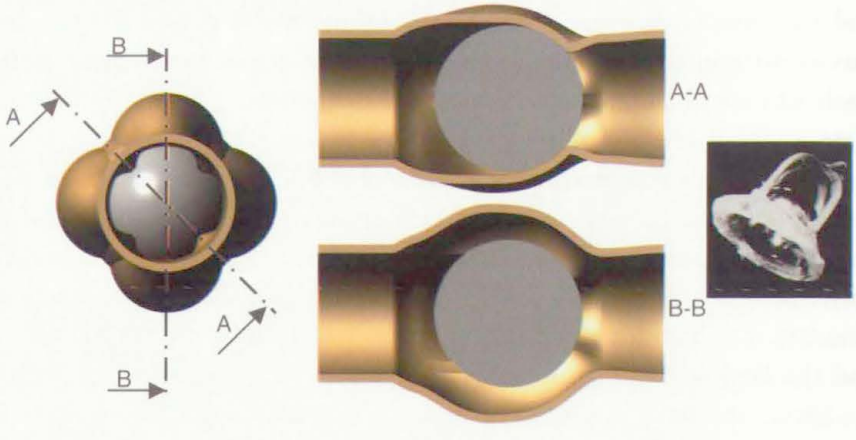

FIGURE 25. CAD view of a ball valve. Struts and stoppers are integrated into the housing.

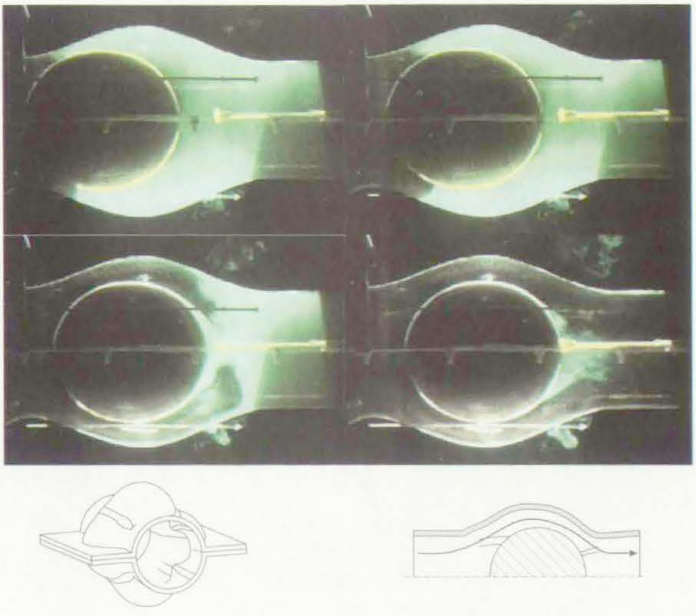

Figure 26. 10:1 model of a ball valve. Downstream of the ball a flow separation appears, but the walls are well washed out.

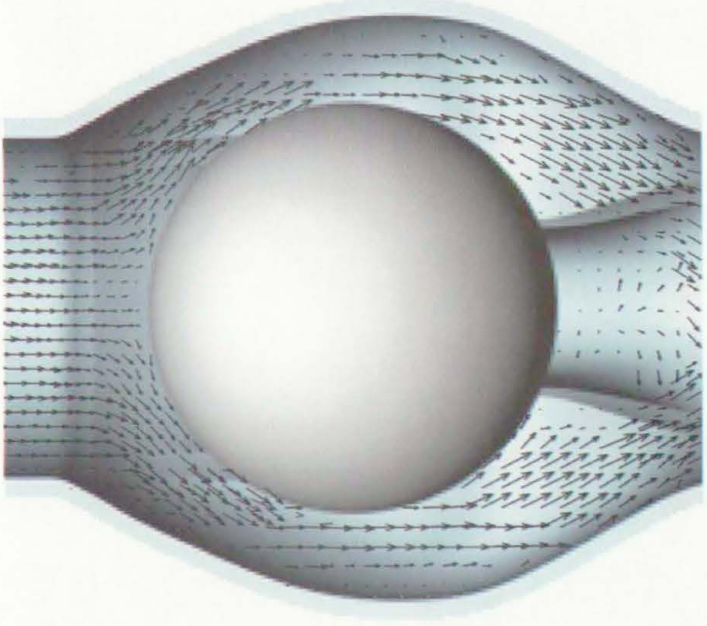

Figure 27. PIV results of the flow field within the ball valve.

FIGURE 28. Inlet and outlet valves which are integrated into a blood pump.

FIGURE 29. Pneumatic blood pump with integrated ball valves.

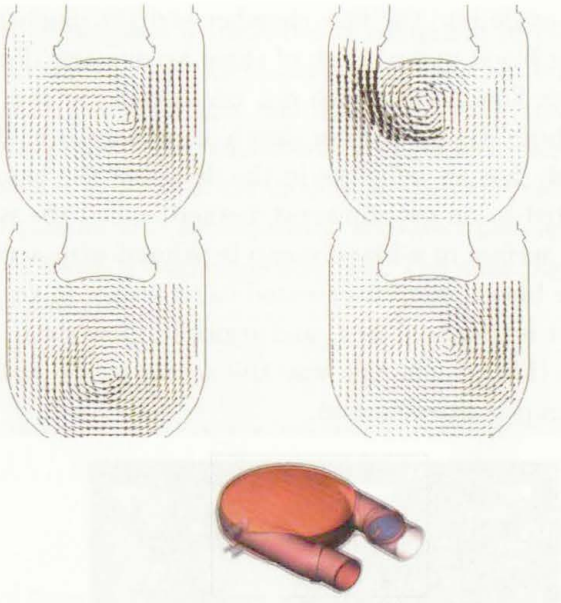

FIGURE 30. Flow field within a pneumatic blood pump on one symmetry plane, obtained with PIV.

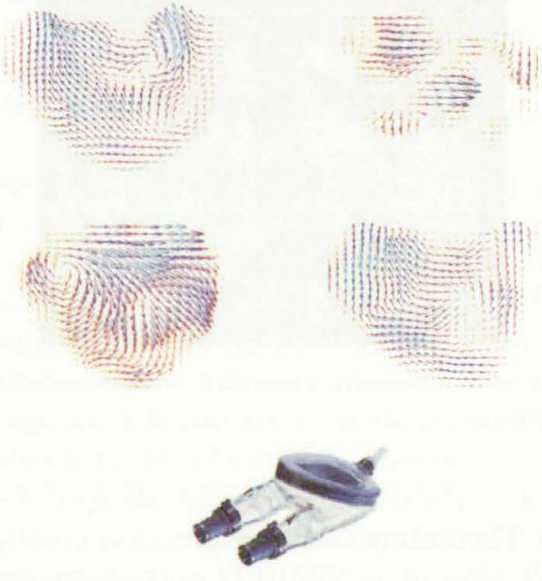

FIGURE 31. Flow field within a pneumatic blood pump with the diagram slanted in respect to the valves, obtained with PIV.

jet impinges at an angle into the flow chamber and the diaphragm acts on only one side of the blood pump. Both of these asymmetric design features create more complex flow fields, which can be observed in the vector field. The average wall shear stress has been shown as influential in the valve design, and it certainly has an influence in the design of the blood chamber. This was investigated in an experimental method, called the paint erosion method. The inner surface of a blood pump is painted with a water soluble paint, and then the blood pump is operated using water. In regions of high shear rate the paint is dissolved first, and regions of low shear rate remain covered with paint (Fig. 32). In this way the action of the wall shear rate inside the blood pump can be assessed.

FIGURE 32. The paint erosion method permits the visualization of the distribution of wall shear stress.

7. Models for Thrombus Generation

From the previous information, the conclusion can be drawn that the generation of a thrombus is the greatest danger for all of these implants. A thrombus is a mass composed of deposited platelets, red blood cells and

fibrin strands. Sometimes a thrombus is composed of platelets alone. This means in effect, that the platelets need to "know" that one has adhered and the next need to recognize this and adhere as well. How is this communication between platelets accomplished? This problem has been investigated with experimental and numerical models. In the experimental model, a fluid composed of plasma and subsequently activated platelets flows towards a glass plate and forms a stagnation flow [13]. The glass plate can be observed through a microscope.

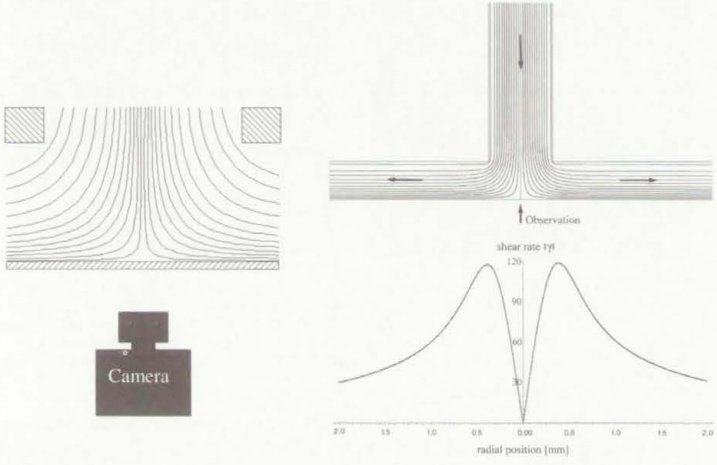

Figure 33. Schematic view of this stagnation flow experiment. The flow field and the resulting shear field at the wall has been computed.

Figure 33 shows the experimental arrangement. The stagnation flow has a central stagnation point where by definition the shear stress is zero. The shear stress increases radially, peaks and then decreases again. The activated platelets come close to the glass wall and some adhere, see Fig. 34.

They form specks of individual thrombi, each of them growing larger with time until they finally combine with each other and form a ring. From the final picture one can conclude that neither in the stagnation point nor at a very large radius does a thrombus form. Both areas coincide with a low or zero shear stress while at a specific shear stress the thrombi are formed massively. This was investigated in a numerical model: a deposited platelet is assumed to give off a messenger molecule like ADP, ATP, or thrombin. With the random walk method the diffusion of these molecules is simulated [14]. In this method one assumes random step which imitates the Brownian movement. A series of steps and a number of molecules form a three dimensional cloud. The

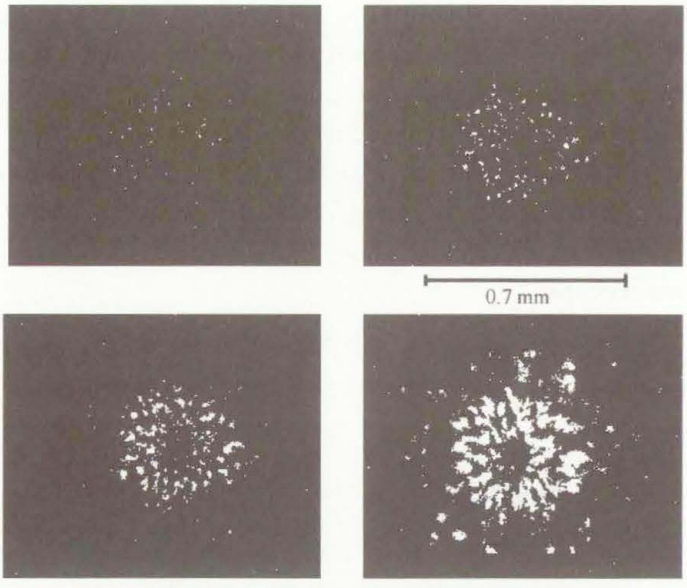

FIGURE 34. Thrombus formation caused by initial platelet adhesion. They grow in size and form larger specks in the form of a ring. The stagnation point in the center remains free of specks.

influence of the flow can be taken into account if at each random step the appropriate velocity is added. The flow field that was assumed has a zero velocity at the wall, and a velocity which increases linearly with the distance to the wall.

Figure 35 shows separate views of the cloud which is formed by diffusion alone, and also by the combination of diffusive and convective motion. The simulation shows that the convection helps to transport the messenger molecules. If one assumes an even stronger flow field than shown in the figure, one would achieve a very long and diluted cloud. From this one can intuitively deduce that diffusion alone does not achieve a transport of a messenger molecule to another platelet, and that a very strong flow does not achieve it either because the cloud becomes too diluted. There must be a combination of diffusive velocity and convective velocity which is favorable for thrombus generation. Since in our experiment the flow field has a radial symmetry, there is a ring of favorable shear rate at which specks of thrombi appear in the experiment. In order to understand this transfer of thrombin molecules to the platelet, a platelet was assumed which is carried by the flow in a certain distance from the wall. When the platelet passes the cloud of molecules

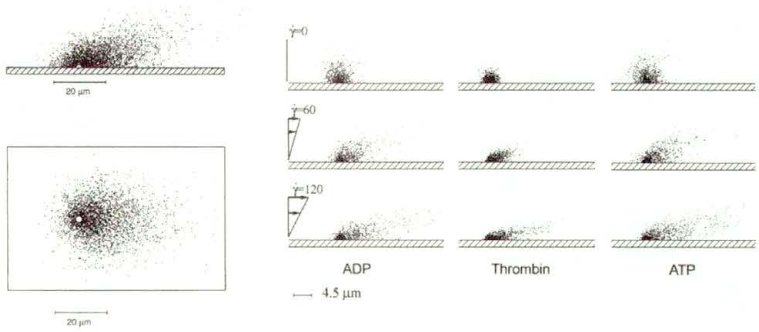

FIGURE 35. In this numerical simulation the random walk method is applied. Random Steps in x, z simulate the Brownian motion of a thromboactive substance. New molecules are emitted and plotted until a cloud is finally formed. If another platelet comes into contact with this cloud, it also becomes activated and emits thromboactive molecules.

which are emitted from the platelet on the wall it comes in contact with these molecules. It becomes activated as well.

In Fig. 36 the number of encountered molecules is plotted as a function of the shear rate and of the distance of the platelet from the wall. These curves show a definite peak, which confirms the observations of the experiment. In

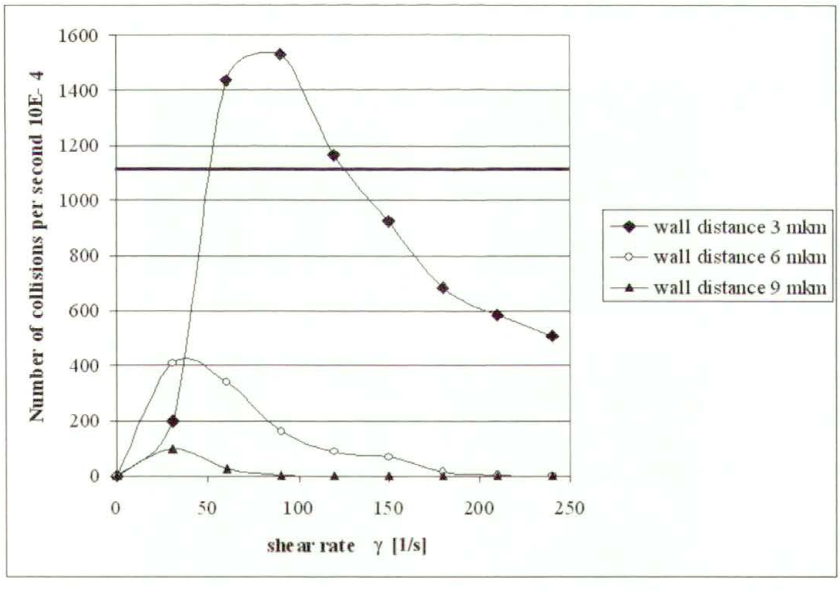

FIGURE 36. Platelets are hit by the molecules depending on the shear rate and the distance to the wall. There is a shear rate at which this occurrence peaks.

other words, there is a combination of the diffusive and convective velocities of the platelet which results in a maximum encounter between molecules and platelet. As a result of this combination the velocity of the platelet is such that thrombus generation is most likely. A cellular automat was designed using this result. As in the original experiment, it has a radial symmetry and at each radius a probability is assigned to each element. This probability is derived from the curve in Fig. 36 and the shear rate in Fig. 33. Another condition is implemented: when by chance a platelet adheres to the plate the probability in the adjacent sections downstream is increased, see Fig. 37. If one runs this cellular automat, the initial speck distribution quickly forms a ring which becomes more solid with time, see Fig. 38.

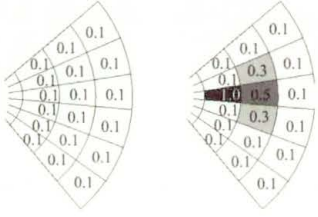

FIGURE 37. The distribution of the probability that a platelet will adhere within the circular grid of the cellular automat (left). If a platelet adheres, the probability in its wake is increased (right).

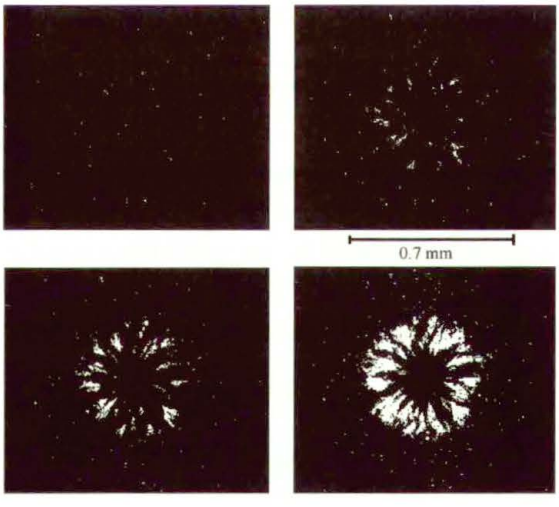

FIGURE 38. Numerical results of the simulation. It agrees well with the experimental results.

When this numerical result is compared to the experimental result, see Fig. 34, one perceives an agreement in regard to shape, distribution, and development. This indicates that the basic mechanism has been modeled correctly. Future work in this method has to include the thrombogenic qualities of the material in the wall and also the dynamic effects because during practical application, the stagnation point and the shear stress field are rarely stable, but instead move around. In addition the shear flow field within artificial elements is far more complex.

8. Conclusion

Modern experimental methods, such as the PIV-method, and numerical methods, such as CFD, have greatly contributed to our understanding of blood flow in the body. However, the unique feature of blood in connection with flow phenomena to coagulate and to become partly solid is not completely understood. We need to integrate the biology of the blood cells, especially the biology of the platelet, into our models. Thrombus generation is one of the most frequent complications found in patients with an artificial blood pump. This prevents these devices from becoming a destination therapy, which is badly needed. Further, little research has been performed on the influence of the flow on the white blood cell. Many of the patients with a VAD suffer from infections, which indicate that white blood cells are affected by the mechanical device. As a result, new experimental and numerical models are needed for a full control of blood in artificial devices.

References

1. P.H. Stone, A.U. Coskun, S.Kinlay, M.E. Clark, M.Sonka, A.Wahle, O.J. Ilegbusi, Y. Yeghiazarians, J.J. Popma, J. Orav, R.E. Kuntz, and C.L. Feldman, *Effect of endothelial shear stress on the progression of coronary artery disease, vascular remodeling, and in-stent restenosis in humans: in vivo 6-month follow-up study*, Circulation., **108**:438–444, 2003.

2. C.R. Huang and W. Fabisiak, *A rheological equation characterizing both the time-dependent and steady state viscosity of worifice human blood*, AIChE Symposium Series, pp.19–21, (1978).

3. R. Virchow, *Phlogose und Thrombose im Gefäßsystem*, [in:] Gesammelte Abhandlungen zur wissenschaftlichen Medizin., Frankfurt am Main: Medinger Sohn und Company, pp.458–612, 1856.

4. P.H. STONE, A.U. COSKUN, Y. YEGHIAZARIANS, S. KINLAY, J.J. POPMA, R.E. KUNTZ, and C.L. FELDMAN, *Prediction of sites of coronary atherosclerosis progression: In vivo profiling of endothelial shear stress, lumen, and outer vessel wall characteristics to predict vascular behavior*, Curr. Opin. Cardiol., **18**:458–470, 2003.

5. A.P. YOGANATHAN, *Cardiac Valve Prostheses*, The Biomedical Engineering Handbook, J.D. Bronzino, [ed.], CRC Press, pp.1847–1870, 1995.

6. G.P. NOON, *Clinical use of cardiac assist devices*, [in:] Heart replacement. Artificial Heart **4**, T. Akutsu, H. Koyanagi, [eds.], Springer, pp.195–211, 1993.

7. K. AFFELD, P. WALKER, and K. SCHICHL, *A ten times enlarged model of artificial heart valve flow*, [in.] 2nd international symposium on biofluid mechanics and biorheology, Springer Verlag, 1990.

8. K. AFFELD, K. SCHICHL and A. ZIEMANN, *Flow Model Studies of Heart Valves*, [in:] New Frontiers in Cardiovasular Engineering, Malaga, Spain: Plenum Press, 1991.

9. K. AFFELD ET AL., *Technical obstacles on the road towards a permanent left ventricular assist device*, Heart and Vessels Suppl. **12**:28–30, 1997.

10. M. LAMBERTZ, K. AFFELD , and A. ZIEMANN, *Untersuchung einer neuen Herzklappe für Herzunterstützungssysteme*, Biomedizinische Technik, **43**(1):514–515, 1998.

11. K. AFFELD, L. GOUBERGRITS, and O. HOLBERNDT, *Novel cardiac assist valve with a purge flow in the valve sinus*, ASAIO J 44, M642–647, 1998.

12. T. TIMMEL, L. GOUBERGRITS, and K. AFFELD, *Optimization and investigation of a novel cardiac assist valve with a purge flow*, Int J Artif Organs, **24**(11):777–783, 2001.

13. K. AFFELD ET AL., *Fluid mechanics of the stagnation point flow chamber and its platelet deposition*, Artif. Organs **1**:722–728, 1995.

14. K. AFFELD, L. GOUBERGRITS, U. KERTZSCHER, J. GADISCHKE, and A. REININGER, *Mathematical model of platelet deposition under flow conditions*, Int J Artif Organs, **27**(8):699–708, 2004.

15. R. COLMAN, J. HIRSH, V. MARDER, and E. SALZMAN, *Hemostasis and Thrombosis: Basic Priciples and Clinical Practice*, (2nd ed.), J.B. Lippincott Company, Philadelphia 1987.